

---

# Influence of depth and 3D crosstalk on blur in multi-view 3D displays

Hyungki Hong (SID Member) 

**Abstract** — Current 3D crosstalk equation was defined from the characteristics of 3D display using glasses. This equation is not suitable for multi-view 3D display with larger view number as it gives the inappropriately large value. In 3D display using eyeglass, double images occur at large depth. But, in multi-view 3D display with larger view number, blur occurs to larger width for the larger depth. Hence, blur phenomenon of multi-view 3D display was investigated to understand the unique characteristics of multi-view 3D display. For this purpose, ray tracing S/W was used to simulate 3D display image seen at the designed viewing distance, to calculate the relative luminance distribution, and to quantify the relation between blur and depth. Calculated results showed that incomplete image separation caused the overlap of multiple view images and the blur. Blur edge width (BEW) was proportional to the horizontal disparity and related to the depth.  $BEWR = (BEW) / (\text{binocular disparity})$  was newly defined, and its usefulness for 3D characterization was investigated. BEW and BEWR might be useful as new measuring items to characterize multi-view 3D display regarding 3D crosstalk.

**Keywords** — autostereoscopic 3D, blur, blur edge width.

DOI # 10.1002/jsid.568

---

## 1 Introduction

Nowadays, 3D TV is commercialized, and people enjoy 3D movies at theater.<sup>1</sup> These applications are based on 3D technologies requiring the special eyeglass. Autostereoscopic multi-view 3D display is under research to enable the user without special eyeglass to perceive the stereoscopic image.<sup>2–7</sup>

In 3D display using eyeglass, incomplete image separation by the left and the right eyes causes the double images or ghost-like artifact that the unintended image of the weak intensity overlaps the intended image. The relative intensity of this unintended image relates to 3D crosstalk. For the larger 3D crosstalk, image separation is worse, and the double images become easier to discern. Hence, large value of 3D crosstalk is considered to cause the degradation of the observed 3D image quality in 3D display using eyeglass.

3D crosstalk of autostereoscopic multi-view 3D display was defined similar to that of 3D display using eyeglass. The definition of multi-view 3D assumes that image of one view is equivalent to the intended image and images of all other views are equivalent to the unintended image.<sup>8–13</sup> For some of multi-view 3D display of large view number, 3D crosstalk was reported to be larger than a few hundred percent.<sup>11–13</sup> Such large value does not accord with the perceived image quality of multi-view 3D display. To

solve this problematic issue, offset crosstalk and 3D pixel crosstalk were recently defined as 3D crosstalk-related property for multi-view display.<sup>12</sup> It is still necessary to define 3D crosstalk-related method which accords with perceived 3D image and is easier to understand.

In multi-view 3D display, effect of incomplete image separation or 3D crosstalk is somewhat different as illustrated in the example of Fig. 1. White area of the sharp boundary and nine regions of different depth were used as 3D input source as illustrated in Fig. 1(a). To make 3D with the different depth, 3D input source of 2D plus-depth format was used. 2D plus-depth format was supported by the commercial 28-view 3D display sample.<sup>14</sup> Photo of the commercial 28-view 3D display with 3D input source of Fig. 1(a) was shown in Fig. 1(b). In Fig. 1(b), the boundaries of the black and white (B–W) were observed to be blurrier with the larger depth even though the B–W boundary of 3D input source was the same irrespective of depth conditions.

This phenomenon of blur did not occur in 3D display using eyeglass. In this respect, phenomenon of blur of multi-view 3D display was investigated in detail to understand the cause and how it related to the depth of 3D source and 3D crosstalk of multi-view 3D display. For this purpose, ray tracing S/W was used to simulate 3D image seen at the user positions, to calculate the relative luminance distribution of these simulated 3D image, and to quantify the relation between blur and depth condition.

---

Received 03/17/17; accepted 07/13/17.

The author is with the Department of Optometry, Seoul National University of Science and Technology, Gongneung gil, Nowon-gu, Seoul 139-743, South Korea; e-mail: hyungki.hong@snut.ac.kr.

© Copyright 2017 Society for Information Display 1071-0922/17/2507-0568\$1.00.

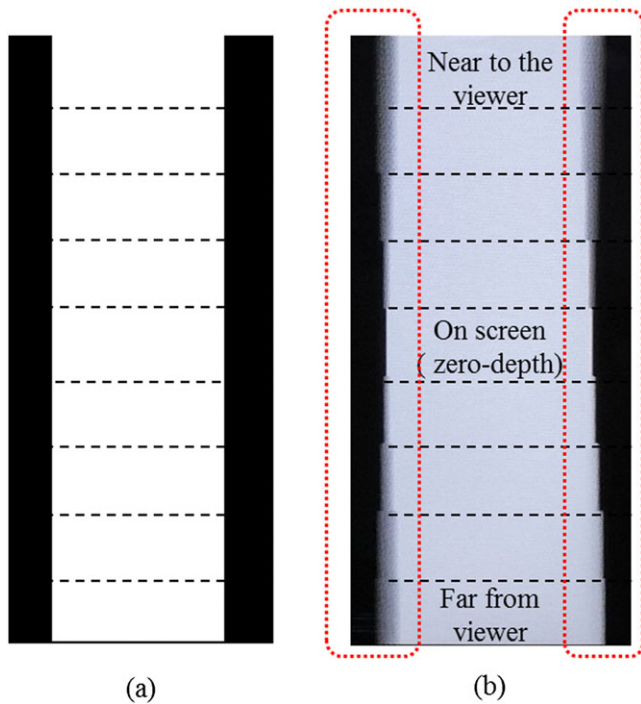


**FIGURE 1** — (a) 3D input source that white area of the sharp boundary on the black background was used with nine regions of the different depth along the vertical direction. (b) Photo of phenomenon of blur in the commercial 28-view 3D display. Upper side and lower side corresponded to the depths in-front and behind 3D display. Dashed lines noted the boundaries of the different depth and were not shown on 3D input source.

## 2 Method

The phenomenon of blur of multi-view 3D display may be schematically explained as Fig. 2. Viewers can see pixels assigned to the multiple views with the varying intensity. As images for the different views are the same at zero depth, overlap of these multiple images is the same as the image for each view as the left side of Fig. 2. In case of non-zero depth, images for the different views are slightly different. Hence, overlap of these multiple images causes the blurring as the right side of Fig. 2(b).

To verify this schematic concept of Fig. 2, spatial luminance distribution for the calculation of 3D crosstalk and the blur at the B–W boundary was simulated. Ray tracing S/W (POVRAY<sup>TM</sup>) was used to simulate the images of autostereoscopic 3D seen at the designed viewing distance (VD).<sup>15</sup> POVRAY has the function to represent the object by the actual length scale, to represent 2D image on the plane by the exact size, and to simulate the refraction by lens. POVRAY also has the function to define the camera angle and the camera position that is equivalent to the position of the observer. To investigate the effect due to view number, configuration of 9-view and 28-view autostereoscopic 3D was selected.<sup>3</sup> Figure 3 illustrates the view map for 9 and 28-view 3D for subpixel configuration of the vertical RGB stripe. Slanted lenticular lens with the angle of arc tan (1/6) was used.

Pixel pitch  $P$  of sample display and the designed VD were selected as 0.372 mm and 2 m. Distance between the adjacent zones at the designed VD were, respectively, selected as 25 and 10 mm for 9 view and 28 view. Other design parameters are listed in Table 1. Figure 4 illustrates the schematic procedure of image simulation. Size of input images was selected as  $640 \times 360$ .  $N$  images for each view were converted into one image where image data for each view were assigned to the corresponding subpixel in consideration of view map using MATLAB<sup>TM</sup>. This image of  $640 \times 360$  size was enlarged to image of  $1920 \times 1080$  size where  $3 \times 1$  pixel of the enlarged image represented each subpixel of RGB. This image of  $1920 \times 1080$  size was displayed on the rectangle of size of  $640P \times 360P = 238.08 \times 133.92$  mm on POVRAY. Each subpixel of flat panel display was surrounded by black matrix of matrix shape. Vertical and horizontal black lines were added on POVRAY to emulate the blocking effect of black matrix. Ratio of these black lines' width to the pixel pitch  $P$  was selected as 0.2. Slanted lenticular lens of specification of Table 1 was also attached on this image of POVRAY. Camera position on POVRAY to capture the simulated image was

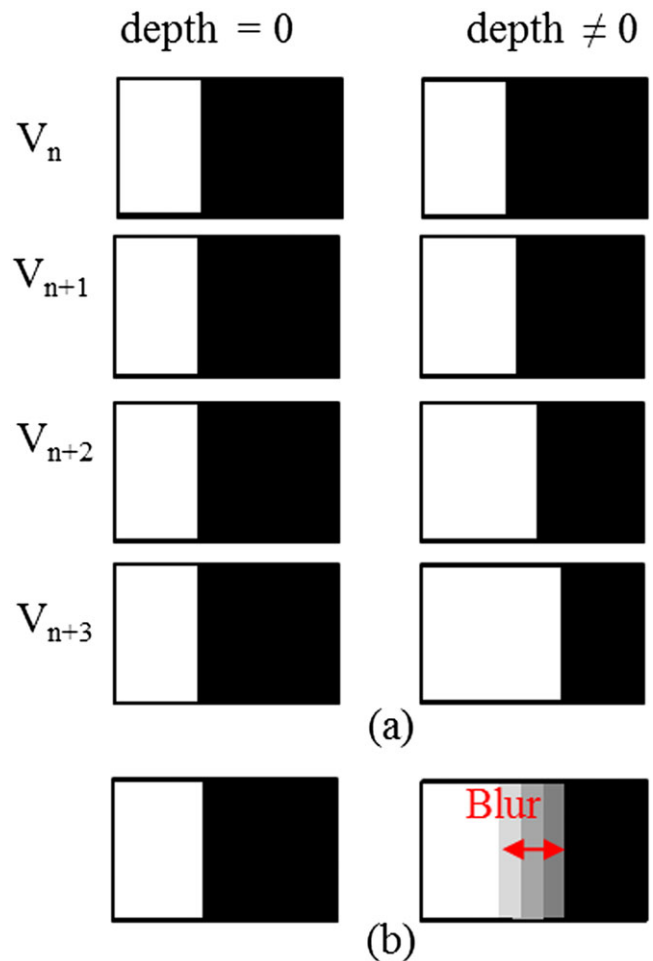


**FIGURE 2** — Schematic concept describing the phenomenon of blur in autostereoscopic multi-view 3D due to overlap of multiple views under incomplete image separation. (a) Image of each view.  $V_n$  represents the image for view  $n$ . (b) Overlapped image seen by the user.

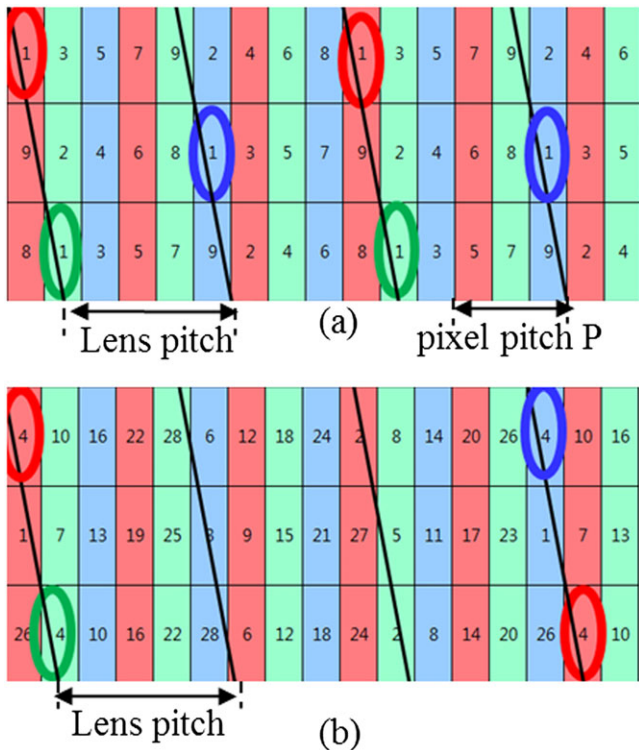


**FIGURE 3** — View map of autostereoscopic 3D displays using the slanted lens for subpixel configuration of vertical RGB stripe at view number of (a) 9 view and (b) 28 view. Solid line represents the lenticular lens array of the slanted angle of  $\arctan(1/6)$ . Rectangles represented red (R), green (G), and blue (B) subpixels.

selected to be equal to the designed VD and kept normal to 3D display surface.

Figure 5(a) illustrates 3D input source to calculate 3D crosstalk for view  $n$ . Image for view  $n$  was the uniform white, while images for other views were the uniform black.<sup>11,12</sup> POVRAY camera position at the designed VD was horizontally shifted by interval of 2.5 mm for the range of 35 cm from the position of P0 which was at the center of the display. At camera angle of  $0.8^\circ$ , the simulated image included about 50 lenticular lens lets along horizontal direction. At each position, 3D image of the size of  $960 \times 540$  was simulated. Relative luminance of each calculated 3D image was calculated by adding the luminance of each pixel of the simulated image. Gamma 2.2 was used to convert the gray level  $i$  of the simulated image to the luminance, using the following equation.

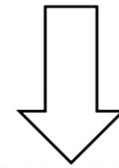
**TABLE 1** — Design parameters for autostereoscopic 3D displays of 9 view and 28 view.

View number	9	28
Distance between the adjacent viewing zones (mm)	25	10
Number of view between interpupillary distance	2.6	6.5
Lens radius (mm)	2.4	2.133
Lens pitch (mm)	0.556408	0.577198
Distance between lens and pixel (mm)	7.2	6.4

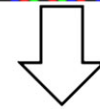
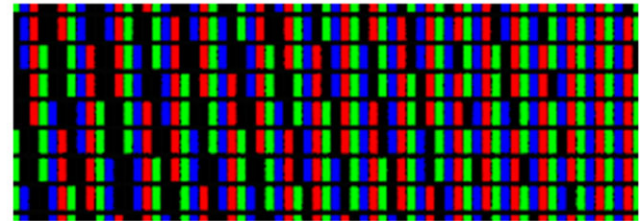
Image for each view for 3D of view number  $N$



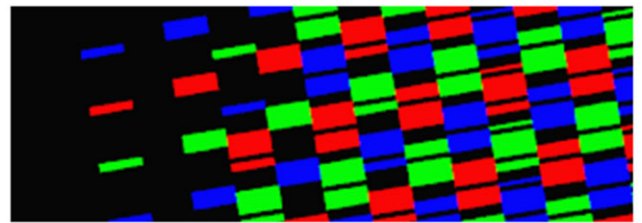
Combine into one image using View map of Figure 3 (MATLAB™)



Add BM for RGB stripe configuration (POVRAY™)



Add lenticular lens (POVRAY)



Capture simulated image at the camera position which is equivalent to the designed Viewing Distance (POVRAY)

**FIGURE 4** — Schematic procedure to simulate the image of autostereoscopic 3D displays seen by the user. MATLAB™ and POVRAY™ are used for the calculation.

$$Lum(i) = \left(\frac{i}{255}\right)^{2.2} \quad (1)$$

To calculate the blur at B–W boundary at the different depth, 3D input source of Fig. 5(b) was used. B–W boundary was shifted by the amount of  $hd$  for image of each view where  $hd$  was the horizontal disparity between images of view  $n$  and  $n + 1$ . BD, the binocular disparity between the images for two eyes, determines the perceived depth. In multi-view 3D, distance between the adjacent two viewing zones at the designed VD can be smaller than interpupillary distance (IPD). In that case, horizontal disparity  $hd$  will be also smaller than BD. If NI is defined as  $IPD / (\text{distance between the adjacent viewing zones})$ , NI is also equal to  $BD/hd$ . As the simulation conditions,  $hd$  was selected as  $0, \pm 5, \pm 10, \text{ and } \pm 15P$  for 9 view and  $0, \pm 2, \pm 4, \text{ and } \pm 6P$  for 28 view. (+) and (–) sign of  $hd$  represented the depth condition behind and in front of 3D display. Position P0 was at the center of the display and at the designed VD.



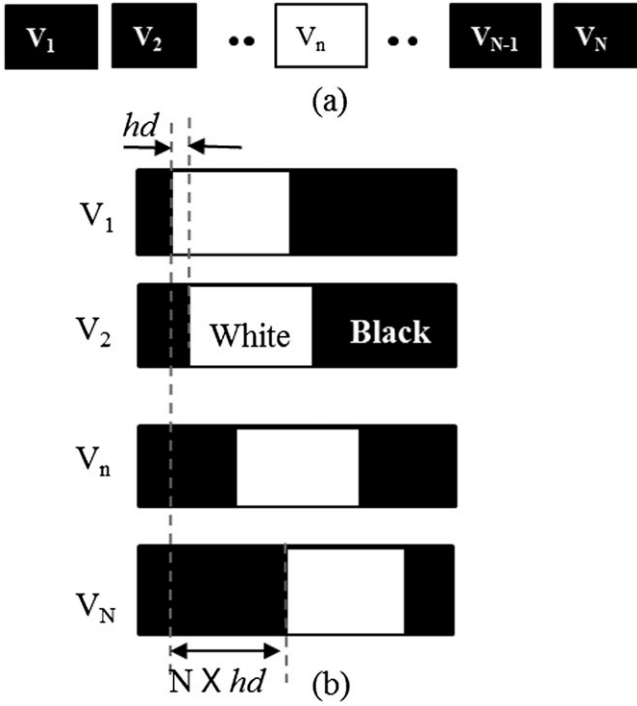


**FIGURE 5** — 3D input source for the simulation of (a) 3D crosstalk and (b) blur at black–white boundary.  $V_n$  represents the image for view  $n$ .  $N$  is the view number, and  $hd$  was defined as the horizontal disparity between the images of view  $n$  and  $n + 1$ .

To observe the blur effect, camera was at the positions P1 and P2. P1 and P2 were horizontally shifted from P0 by  $-25$  and  $25$  mm. Size of the simulated 3D image for the blur was  $3840 \times 2160$  with POVRAY camera angle of  $5^\circ$ . From the simulated images of different  $hd$ , the luminance distribution at B–W boundary along the horizontal cross section was calculated by averaging the luminance of each pixel along the vertical directions.

### 3 Result and analysis

Figure 6 illustrates the average luminance of each view at the designed VD using 3D input source of 3D crosstalk of Fig. 5(a). POVRAY camera positions were horizontally shifted to emulate the shift of the user position. Average luminance was calculated adding the luminance of each pixel of the image at each position for view  $n$ . In ideal lens, this luminance distribution can be roughly derived from the view map of Fig. 3 that the slanted line of the lens on the multiple subpixel determines the size of overlap of views. Distances between two adjacent luminance peak for view  $n$  and  $n + 1$  of Fig. 6 were calculated to be 25 mm for 9-view 3D and 10 mm for 28-view 3D. These are equal to the designed values. Overlap of luminance of views was larger for 28 view than 9 view. To calculate 3D crosstalk, the following equation was used.<sup>12</sup>

$$3D \text{ crosstalk} = \frac{\sum_{i=1}^N L_i - \max(L_i)_{i=1}^N}{\max(L_i)_{i=1}^N} \times 100\% \quad (2)$$

$N$  is the view number, and  $L_i$  is the luminance when view  $i$  is white and all other views are black. Using Eq. (2), 3D crosstalk at peak position of each view was calculated to be 51% for 9-view 3D but 396% for 28-view 3D. 3D crosstalk of such value larger than few hundred percent was criticized to be unrealistic. If the intensity of unintended image was much larger than the intensity of the intended image, the viewer would not identify the intended image. However, the viewer could still perceive 3D even if 3D crosstalk was more than a few hundred percent. Hence, the current definition and the distinction of the intended and unintended image was inappropriate to multi-view 3D display of large view number. Therefore, new definition is needed to characterize the incomplete image separation or 3D crosstalk for autostereoscopic 3D of large view numbers.

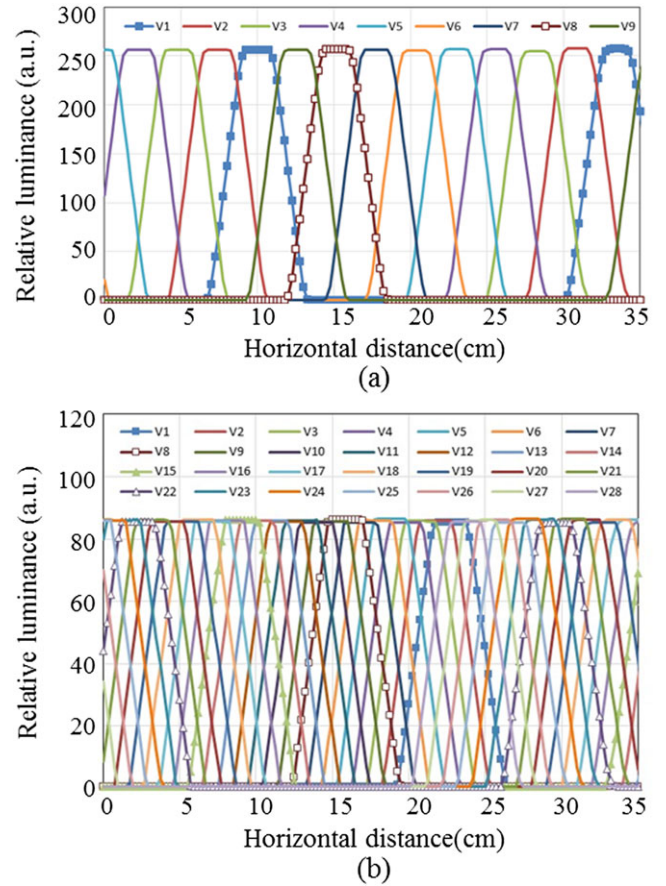


**FIGURE 6** — Simulated average luminance at the designed viewing distance using 3D input source of 3D crosstalk for (a) 9 view (b) 28 view. Horizontal axis represents the distance of POVRAY camera position from P0 along the horizontal direction. Vertical axis represents the average luminance of each calculated image.

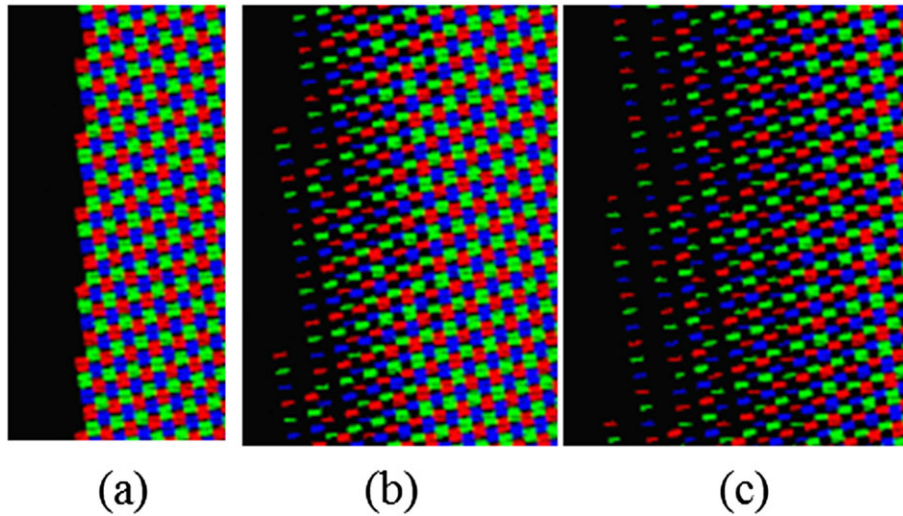


**FIGURE 7** — Black–White boundaries of simulated 3D image of 28 view using 3D input source of blur for  $hd$  of (a)  $0P$ , (b)  $4P$ , and (c)  $8P$ . Pixel pitch  $P$  is  $0.372$  mm. Dashed gray line represents the position of the horizontal cross section.

Figure 7 illustrates B–W boundaries of the simulated image of 28-view 3D using 3D input source of Fig. 5(b) at the various  $hd$  condition. At  $hd = 0P$ , the bright area of each subpixel enlarged by lenticular lens were roughly the same. But when  $hd$  was not zero, the bright area of each subpixel was different around B–W boundary. Hence, B–W boundaries became less sharp for non-zero value of  $hd$ . Figure 8 illustrates the luminance along horizontal cross section of the simulated images for different  $hd$ . For 9-view 3D, a discrete change occurred at B–W boundary, and this width increased with larger  $hd$ . But for 28-view 3D, luminance change at B–W boundary was more gradual and the width of B–W boundary was larger for the larger  $hd$ . The trend of Fig. 8(b) accorded with the photo of the commercial 3D display of Fig. 1(b). The calculated result for the negative value of  $hd$  was the same, although the luminance curves of non-zero  $hd$  were located to the left side of the curve at  $hd = 0$ .

The difference between 9-view and 28-view 3D can be explained by the overlap of luminance distribution of Fig. 6. Figure 9 illustrates the partial result of Figs. 6 and 8 at POVray camera position of  $P_0 = 0$  mm. For 9-view 3D, this position corresponds to the viewing zone of view 5 where peak luminance of view 5 is located. At this position, subpixel for image of view 4 can be also seen as the luminance for view 4 is not zero. As images of views 4 and 5 are different by the amount of  $hd$ , overlapped images of views 4 and 5 will cause the discrete change of  $hd$  at BW boundary. In case of 28 view, the position of  $P_0$  corresponds to the viewing zone of view 24. Luminance of views 21–27 is not zero at this position. Hence, the observed 3D images are overlaps of images for views 21–27 with the different intensity. At non-zero  $hd$ , each discrete step becomes less noticeable, and boundary at 28-view 3D is no longer clearly defined, in contrast to the result of 9 view.

To characterize the gradual luminance change at B–W boundary, blur edge width (BEW) for multi-view 3D display

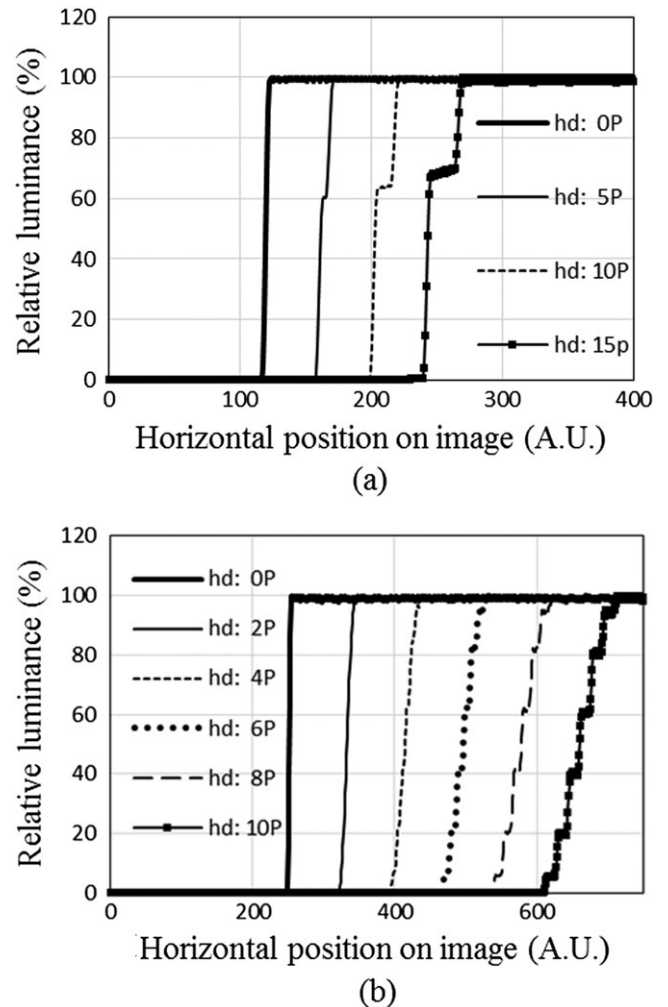


**FIGURE 8** — Luminance along horizontal cross section of simulated image using 3D input source of blur for (a) 9-view and (b) 28-view 3D. Numbers behind  $hd$  represent the size of horizontal disparity between images of two adjacent views. Horizontal axis represents the horizontal position on the calculated image in arbitrary unit. Vertical axis represents the normalized luminance at horizontal cross section of the calculated image.

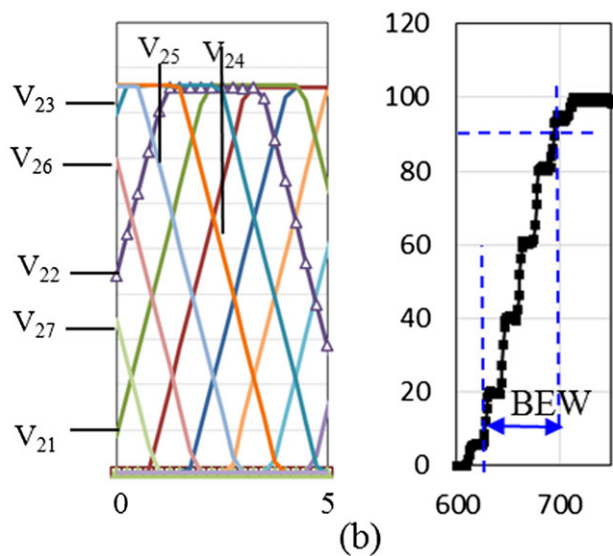
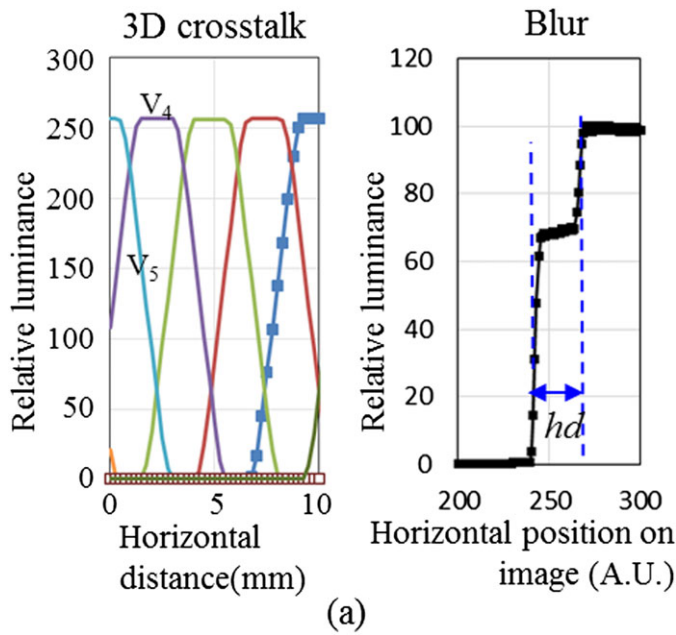


**FIGURE 9** — Results for 3D input source of 3D crosstalk and bur at (a) 9 view,  $hd = 15P$  and (b) 28 view,  $hd = 10P$ . Blur edge width is defined as the distance between the position of 10 and 90% luminance.

was newly proposed as the distance between the positions of 10 and 90% luminance. As the shapes of blurred boundary are diverse, characterization of the phenomenon of blur is not simple. For example of moving edge blur, various methods had been proposed, and the use of the interval between 10 and 90% was one of the methods.<sup>11</sup> Similarly, methods other than 10–90% interval can be used to characterize the phenomenon of blur in multi-view 3D display. Figure 10 illustrates BEW for 3D of 28 view which was calculated from the result of Fig. 8. BEW increased almost linearly for the increase of  $hd$ .

In the previous result, BEW was measured in arbitrary unit (AU). In the measurement of the actual multi-view 3D display using camera or 2D light-measuring device), actual size of

BEW needs to be obtained from 2D luminance distribution. Figure 11(a) illustrates the B–W boundary where the horizontal position of camera was at  $P1 = -25$  mm and  $P2 = 25$  mm for 28-view 3D. The distance between  $P1$  and  $P2$  was selected as 50 mm. The distance  $D1$  between the positions of 50% luminance of two B–W boundary at  $P1$  and  $P2$  was 198 AU for  $hd = 0P$  in Fig. 11(a). As there is no disparity for  $hd = 0P$ , the camera movement of 50 mm causes the shift of B–W boundary by the amount of  $D1$  (AU). Hence, this ratio of (distance between two cameras in length unit)/(distance of boundaries of zero depth in AU) can be used to obtain the actual size of BEW. For example of Fig. 11(a), this ratio was  $50 \text{ mm}/(198 \text{ AU})$ . As BEW at  $hd = 6P$  was 40 AU, this value was equal to  $(40 \text{ AU}) \times (50 \text{ mm}/198 \text{ AU}) = 10.1 \text{ mm}$  in actual size.

There are various 3D image formats for 3D display, and the various image processes are often applied by hardware of 3D display. Knowing the exact value of disparity between images on the 3D display is not always possible. Yet, 3D images observed at two different position can be used to determine the disparity. In example of Fig. 11(b),  $hd$  was selected to be 6P. When the horizontal position of luminance curve measured at  $P1$  position was shifted by  $D1$ , B–W boundary of  $hd = 0P$  of positions  $P1$  and  $P2$  were located at the same position as illustrated in Fig. 11(b). In Fig. 11(b), the distance between the positions of 50% luminance of B–W boundary of non-zero  $hd$  for camera positions of  $P1$  and  $P2$  was defined as  $D2$ . As  $D2$  was 44 AU for  $hd = 6P$ , this value was equal to  $44 \text{ AU} \times (50 \text{ mm}/198 \text{ AU}) = 11.11 \text{ mm} = 29.87P$ . Distance between the adjacent zone for 28-view 3D was designed to be 10 mm. As images seen at positions  $P1$  and  $P2$  were separated by 50 mm,  $D2$  was caused by view  $n$  and view  $n + 5$ .  $D2$  divided by the number of views between positions  $P1$  and  $P2$  was equal to the difference between two adjacent viewing zones. In the example,  $D2/5$  was calculated to be  $5.97P$  which was approximately the same as  $hd = 6P$  of 3D input source.  $D2$  was derived from 3D images observed at two different positions without any information of  $hd$ .

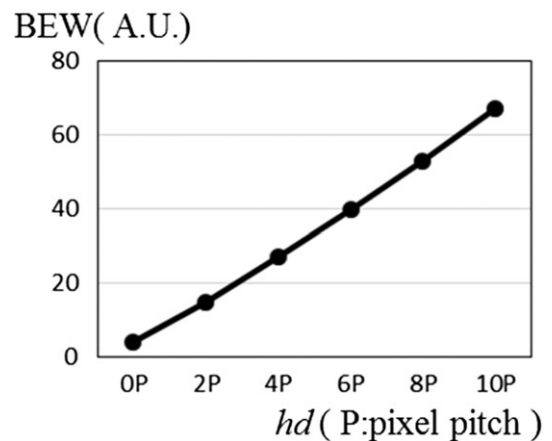
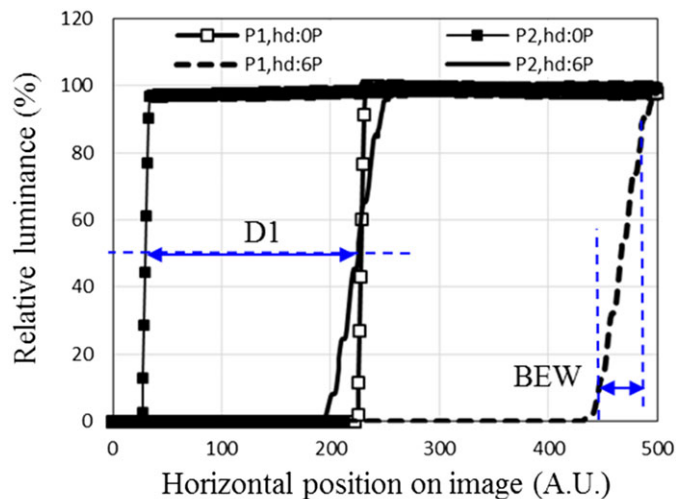
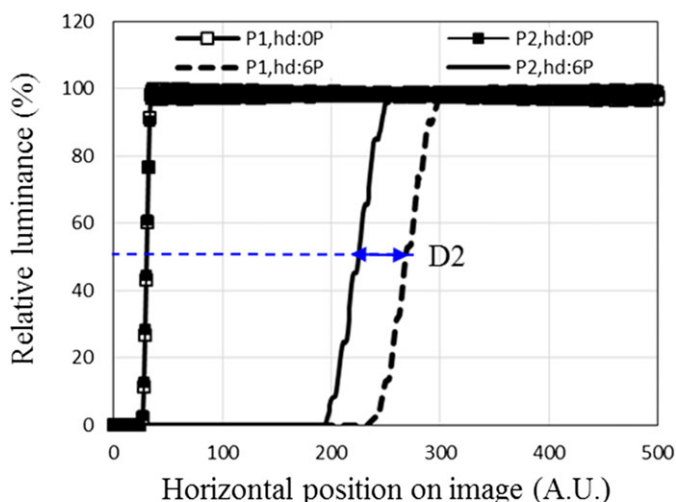


**FIGURE 10** — Blur edge width derived from the simulated image using 3D input source of blur at the different  $hd$ . Horizontal and vertical axis represent  $hd$  of 3D input source and BEW in arbitrary unit, respectively.





(a)



(b)

**FIGURE 11** — (a) Luminance at horizontal cross section of simulated image using 3D input source of blur for 28 view at camera positions of P1 and P2 which are horizontally 50 mm apart. (b) The same luminance where the result for camera position P1 is horizontally shifted by the amount of D1. Horizontal axis represents the horizontal position on the calculated image. Vertical axis represents the normalized luminance at horizontal cross section of the calculated image.

Hence, using 3D images observed at two different positions,  $hd$  can be determined.

In viewing 3D, the binocular disparity between the images for two eyes determines the depth. As  $NI = IPD / (\text{distance between the adjacent two viewing zones}) = (BD) / hd$ , the size of  $hd$  is affected by  $NI$  as well as the depth. For autostereoscopic 2 view 3D,  $NI$  is 1 and  $BD$  is equal to  $hd$ . When  $NI$  is near 1, the distinction of the intended and unintended images is meaningful, and incomplete separation between the viewing zones causes the user to perceive the double image. For larger  $NI$ ,  $hd$  becomes smaller. In the selected example,  $NI$  was selected to be 6.5 for 28 view and 2.6 for 9 view. When  $NI$  is much larger than 1 like the example of 28-view 3D, image difference between the adjacent viewing zones is small, and the distinction of the intended

and unintended images become meaningless. In that case, the current definition of 3D crosstalk for multi-view 3D would be inappropriate. The phenomenon of blur directly affects the image quality of the observed 3D image. User will be easier to understand BEW, compared with the inappropriately large value of crosstalk of multi-view 3D display.

The metric without the dependence on  $hd$  or 3D input source might be useful as well. BEW related to the average luminance of each view at the designed VD as illustrated in Figs. 6 and 9, while optical 3D design of slanted lens angle, pixel pitch, lens pitch, and view map determined the average luminance. BEW was also proportional to  $hd$  of 3D input as illustrated in Fig. 10. If  $C1$  was defined as  $(BEW / hd)$ ,  $C1$  was independent of  $hd$  and related to the optical 3D design. As the perceived depth by two eyes is determined not by  $hd$  but by  $BD = (NI \times hd)$ , BEW ratio (BEWR) is newly defined as

$$\begin{aligned} \text{BEWR} (\%) &= \text{BEW} / \text{BD} = (C1 \times hd) / (NI \times hd) \\ &= C1 / NI \end{aligned} \quad (3)$$

Equation (3) of BEWR is independent of  $BD$  of 3D input source and includes  $C1$  which related to 3D design. In Fig. 10 of 28-view 3D and  $NI = 6.5$ ,  $C1$  and BEWR were calculated to be 454 and 70%. If  $NI$  is changed to 10 for the same configuration of Fig. 3(b),  $C1$  is unchanged, and overall shape of luminance distribution of Fig. 6(b) is the same except that the distances between the luminance peaks reduce to 6.5 mm. To induce the same depth at  $NI = 6.5$  and 10,  $BD$  had to be the same but  $hd = NI / BD$  is dependent on  $NI$ . Hence, BEWR for  $NI = 10$  is 45.4%, which is smaller than  $\text{BEWR} = 70\%$  for  $NI = 6.5$ . Smaller 3D crosstalk had been known to be preferable. As larger  $NI$  in multi-view or super multi-view 3D display causes the smaller BEWR, the effect of  $NI$  on BEWR accords with the existing preference of 3D crosstalk.

## 4 Conclusion

Image simulation by ray tracing S/W was used to investigate the phenomenon of blur in autostereoscopic multi-view 3D display. Blur was observed when the view number was very large or the number of viewing zones between IPD was much larger than 1. Blur is caused by overlap of multiple images due to the incomplete image separation of views at the designed VD.

From the example of image simulation of 28-view 3D, BEW and BEWR were newly proposed and investigated. Also, measuring procedure that uses the camera position movement was described to derive the disparity among images of the different viewing zones. As BEW directly affects the observed 3D image, the value of BEW will be easier to understand for the user. Like the current definition of 3D crosstalk, BEWR is represented in the unit of the percentage

and provides the more realistic value. BEWR also includes the effect due to 3D lens design and the size of interval of each viewing zone.

The current definition of 3D crosstalk was defined assuming the distinction of the distinction of the intended and unintended images. This definition was not suitable for multi-view 3D display where the phenomenon of blur occurred. BEW and BEWR might be useful as new measuring items to characterize the performance of 3D regarding 3D crosstalk.

---

## Acknowledgment

This research was supported by the Research Program funded by the Seoul National University of Science and Technology.

---

## References

- 1 The illustrated 3D movie list, "The illustrated 3D HDTV list", <http://www.3dmovielist.com>, accessed Feb,(2014).
- 2 T. Okoshi, *Three Dimensional Images Techniuqes*. Academic Press, New York, (1976).
- 3 C. van Berkel, "Image preparation for 3D-LCD," *Proceedings of SPIE*, **3639**, 84–91 (1999).
- 4 B. Javidi and F. Okano, *Three-Dimensional Television, Video and Display Technologies*. Springer, New York, (2002).
- 5 J. Y. Son and B. Javidi, "Three-dimensional imaging method based on multiview images," *Journal of Display Technology*, **1**, 125–140 (2005).
- 6 H. K. Hong and M. J. Lim, "Determination of luminance distribution of autostereoscopic 3-D displays through calculation of angular profile," *Journal of SID*, **18**, 327–335 (2010).

- 7 Y. Takaki, "Multi-view 3-D display employing a flat-panel display with slanted pixel arrangement," *Journal of SID*, **18**, 476–482 (2010).
- 8 M. Salmimaa and T. Järvenpää, "3-D crosstalk and luminance uniformity from angular luminance profiles of multiview autostereoscopic 3-D displays," *Journal of SID*, **16**, 1033 (2008).
- 9 A. Yuuki *et al.*, "Influence of 3-D cross-talk on qualified viewing spaces in two- and multi-view autostereoscopic displays," *Journal of SID*, **18**, 483–493 (2010).
- 10 A. Abileah, "3-D displays—technologies and testing methods," *Journal of SID*, **19**, 749–763 (2011).
- 11 ICDM(International Committee for Display Metrology), <http://www.icdm-sid.org/downloads/idms1.html>, accessed Dec, (2016)
- 12 International Electrotechnical Commission "IEC 62629-22-1: 3D display devices—part 22-1: measuring methods for autostereoscopic displays-optical, Edition 2"(2016)
- 13 S. M. Jung *et al.*, "New characterization of 3D performance for multi-view autostereoscopic displays," *SID Symposium Digest*, **43**, 1155–1158 (2012).
- 14 Skymedia 28view"skymedia.com", accessed Nov,(2016)
- 15 POVRAY"www.povray.org", accessed Dec,(2016)



**Hyunki Hong** is an associate Professor at Department of Visual Optics, Seoul National University of Science and Technology since 2010 and a member of SID. He received his B.S. in Physics in Seoul National University and PhD in Physics from Korea Institute of Science and Technology (KAIST). After receiving PhD in 1998, he joined LG Display (at that time LCD division of LG Electronics) and worked for the performance improvement and the performance characterization of LCD and 3D display until 2010. His research interest is human factors related to displays such as 3D and VR.